

Macroscopic Spin-Orbit Interaction through Strong-Field Pumping of Inhomogeneously Aligned Molecular Ensemble

Uriel Zanzuri*

*The Raymond and Beverly Sackler Faculty of Exact Sciences
Tel Aviv University, Tel Aviv 6997801, Israel*

Sharly Fleischer 

*Physical Chemistry Department, Raymond and Beverly Sackler Faculty
of Exact Sciences, Tel Aviv University, Tel Aviv 6997801, Israel*

Tamar Seideman 

Department of Chemistry, Northwestern University, Evanston, Illinois 60208, USA

Eldad Yahel, Amir Natan † and Alon Bahabad ‡

The School of Electrical Engineering, Tel Aviv University, Tel Aviv 6997801, Israel

(Dated: February 13, 2026)

We study the strong-field interaction of a helical bi-chromatic pump with an anisotropic and inhomogeneous molecular system in the form of planar distribution of radially aligned molecular ensemble. This setting gives rise to macroscopic spin-orbit interaction where High Harmonic radiation is emitted while imbued with Orbital Angular Momentum (OAM) whose sign is directly dictated by the helicity of the pump field. We demonstrate this phenomenon in ensembles of H_2^+ and N_2 molecules with Time-Dependent Density Functional Theory (TDDFT) simulations.

Introduction. High Harmonic Generation (HHG) is an extreme nonlinear optical process in which an ionizing ultrashort pump field interacts with a medium. HHG was studied extensively within the gas phase since 1988 [1, 2] with particular attention to interaction with aligned molecules [3–7]. These studies have revealed effects associated with molecular symmetry [4], the dependence of HHG amplitude and polarization state on the molecular angle [6] and more. The vast majority of these works considered effects explained at the single emitter level, which entails a homogeneous molecular ensemble - that is - the alignment of all molecules is the same everywhere within the plane of interaction with the HHG pump field. Here we consider the strong-field interaction of a pump field with a molecular ensemble that is both inhomogeneous and anisotropic - the molecules are all aligned but, the alignment direction is a function of the position in space. This kind of symmetry is known to induce macroscopic spin-orbit coupling and was employed in various devices [8, 9], which essentially are an embodiment of the q-plate [9], the first such device suggested and implemented using liquid crystal substrate. In a macroscopic spin-orbit coupling, also known as spin-orbit interaction [8], the spin angular momentum (SAM) of light, manifested by the polarization state of light, is coupled to the orbital angular momentum (OAM) of light. The latter is linked to the presence of a helical phase front in the field's amplitude

of the form $\exp(il\theta)$ where l is known as the topological charge. Light impinging on a q-plate can acquire OAM (or change its value) in a way that is dependent on the value of its SAM. The use of a molecular q-plate was recently demonstrated in three key works. Trawi et al. [10] successfully exploited a molecular q-plate to create a molecular quantum interface for storing and retrieving OAM. Xu et al. [11] created a highly efficient, broadband molecular wave plate for generating ultrashort optical vortices across UV-IR wavelengths. Voisine et al.[12] have demonstrated that the vortex beam can be read-out 'on demand' using rotational echo scheme. Here we extend the application of the molecular q-plate into the strong-field regime to manipulate HHG. Explicitly, we show that when the molecular q-plate is pumped with a bi-chromatic helical pump consisting of circularly polarized fields, the emitted high harmonics carry OAM whose polarity depends on the SAM of the pump components.

Real-Time TDDFT (RT-TDDFT) [13] is a powerful method for calculating the non-linear response of electrons within molecules to a strong laser field in the semi-classical approximation. RT-TDDFT was used in many works to calculate the response to a linear [14–16], circular [17, 18] and bi-chromatic circularly polarized (BCCP) laser field [19]. In this work, we use RT-TDDFT to calculate the response of aligned H_2^+ and N_2 molecules to BCCP laser. Accounting for the emission from the entire radially aligned molecular ensemble, we find that the far field radiation carries OAM at selected harmonics, providing new means for generating OAM beams across various frequencies of interest.

* urielzanzuri@mail.tau.ac.il

† amirnatan@tauex.tau.ac.il

‡ alonb@tauex.tau.ac.il

Methodology. In our theoretical framework, we model the interaction of a gas layer composed of symmetric di-atomic homonuclear molecules radially aligned within a constrained spatial dimension. The molecular layer's thickness is small to mitigate phase mismatch phenomena within the medium, [20]. De facto, the medium consists of a single layer of these molecules.

The molecules are pre-aligned via the response elicited by a strong laser pulse [21–24], where the alignment is primarily driven by the induced dipole interaction, where $\hat{V} = -\frac{1}{4}|E|^2(\Delta\alpha\cos^2\theta + \alpha_{\perp})$. Here, $\Delta\alpha = \alpha_{\parallel} - \alpha_{\perp}$ is the anisotropic molecular polarizability, E is the electric field applied on the molecule, and θ is the angle between the molecular axis and the field polarization axis.

The aligning beam is configured as a radial linear vector beam — a beam whose polarization state is linear at every point but aligns radially around the center of the beam. This specific polarization state is achievable, for example, by transmitting a uniformly linearly polarized beam through a q-plate characterized by a topological charge of $q_p = \frac{1}{2}$ [9].

Following the interaction with the aligning pulse, the molecules realign in a periodic manner known as 'rotational revivals' [21, 25, 26], i.e. the aligned molecules can be further interrogated under field-free conditions by the HHG pump. The duration of each alignment event depends on the molecular moment of inertia, the temperature of the ensemble, as well as on the parameters of the alignment pulse (duration and intensity) [21, 27], in the range of a few tens of fs for small diatomics and up to a few ps for large ones [28, 29]. We therefore treat the 'aligned' molecules as static rotors during their interaction with the ultrashort HHG pump field (chosen as much shorter than the duration of alignment) for brevity.

The simulations were conducted at two distinct levels: microscopic and macroscopic. The microscopic simulations utilize RT-TDDFT through the Bayreuth version of the PARSEC package [30–33]. These simulations explore the dynamic response of aligned diatomic molecules subjected to a BCCP HHG pump field at varying relative alignment angles.

The HHG pump field is configured as the composite of two counter-rotating circularly polarized field components, oscillating at the fundamental frequency ω_0 and its second harmonic $2\omega_0$:

$$\mathbf{E}_1(t) = \frac{1}{\sqrt{2}}E_0f(t)[\hat{\mathbf{e}}_y\cos(\omega_0t) + \hat{\mathbf{e}}_z\sin(\omega_0t)] \quad (1)$$

$$\mathbf{E}_2(t) = \frac{1}{\sqrt{2}}E_0f(t)[\hat{\mathbf{e}}_y\cos(2\omega_0t) - \hat{\mathbf{e}}_z\sin(2\omega_0t)] \quad (2)$$

where $f(t)$ represents the envelope of the pulse. Here the overall field is a right-handed BCCP field for which the fundamental is Right-Handed Circularly polarized (RHC) and the second-harmonic is Left-Handed Circularly polarized (LHC). The BCCP field, known for its

efficiency in generating circularly polarized HHG from atoms [34], possesses a helical structure. The helicity of this field can be altered by exchanging between the circular polarization helicity of its two components. The trajectory described by the tip of this field in space, along with a schematic of an aligned molecule interacting with it, is depicted in Fig. 1.

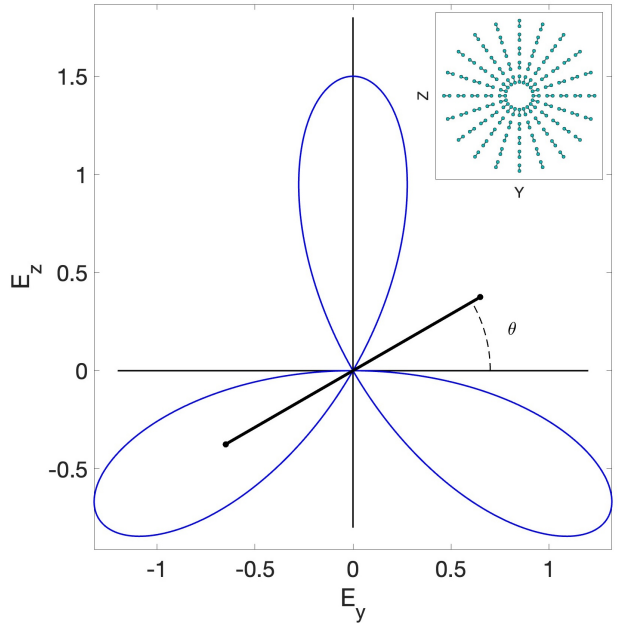


FIG. 1. A schematic cross-section of a bi-chromatic laser field interacting with a di-atomic molecule, oriented at an angle θ to the bichromatic field. The inset illustrates the molecular ensemble orientation.

For the TDDFT simulations, the evolution of Kohn-Sham (KS) orbitals is approximated using a fourth-order Taylor expansion combined with a predictor-corrector method [32]. These simulations provide the dynamics of the orbitals under the influence of the laser field.

We focus on the induced dipole components along the y and z axes. From the Fourier transform of the time-dependent dipoles, we derive the harmonics spectrum in both the y and z directions. A custom script has been developed to locate and record the complex value of each harmonic peak. The magnitude of the peak represents the absolute value, indicative of the point source amplitude, whereas the angle provides the phase of this source. The mathematical representation of the time-dependent dipole and its Fourier transformation is given by:

$$\vec{d}(t) = \int d\vec{r}\vec{r}\rho(\vec{r}, t), \quad \vec{d}(\omega) = \frac{1}{T} \int_0^T dt e^{-i\omega t} \vec{d}(t) \quad (3)$$

where $\rho(\vec{r}, t)$ denotes the electron density at position \vec{r} and time t , $\vec{d}(t)$ represents the time-dependent dipole, and $\vec{d}(\omega)$ is its Fourier transform in the frequency domain.

We simulated the interaction for both H_2^+ and N_2 molecules. Technical information about the simulation parameters is given in section II of the supplementary material (SM). For H_2^+ , which contains only a single electron, the simulation employs a pure Time-Dependent Schrödinger Equation (TDSE) approach, capturing the dynamics of the electron under the applied field. N_2 , being a multi-electron system, necessitates the use of Time-Dependent Density Functional Theory (TDDFT) incorporating the asymptotically corrected van Leeuwen and Baerends (LB) exchange functional [35], which previously was shown to predict a realistic ionization potential for N_2 [36].

The macroscopic part of the simulation uses the outcomes of the microscopic analysis as an input for propagating the dipole radiation emitted from the molecules in the ensemble to the far field. The following results highlight how the macroscopic response mediates a spin-orbit coupling. Specifically, the OAM state of the far-field radiation is shown to depend on the helicity of the pump, which is directly dictated by the SAM of its two components (fundamental and second harmonic).

Results. We begin by presenting the TDSE microscopic simulation results for the H_2^+ molecule, which serves as an ideal numerical system for studying the generated dipole moment as a function of its alignment relative to the bi-chromatic electric field orientation, as illustrated in Fig. 1.

A representative case is displayed in Fig. 2, where the molecule is aligned at a relative angle of $\theta = 0^\circ$ to the bi-chromatic electric field. This example reveals that harmonics of even order, which are forbidden in linear polarization, are generated under the counter-rotating bi-chromatic field [37].

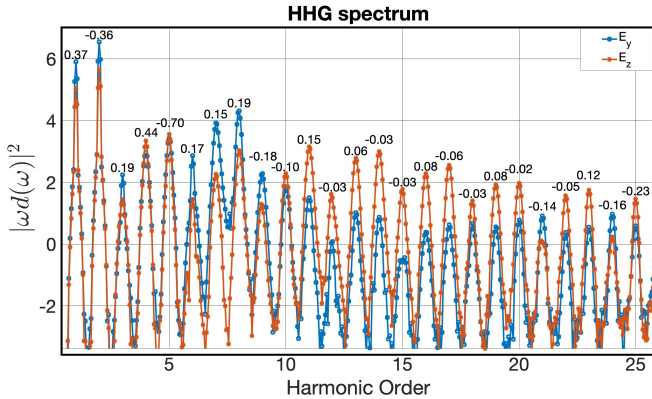


FIG. 2. Harmonic spectra of H_2^+ for $\theta = 0^\circ$ (as defined in Fig. 1) under a bi-chromatic laser field. The ellipticity for each harmonic order is shown above the peaks, the sign of which represents the handedness of the field.

Our main interest here is in systems that can be readily tested in the laboratory. As such, the N_2 molecule, which has served as a case study in most experiments on HHG from molecules, is a useful example explored in

the remainder of the paper (additional results of H_2^+ are provided in sections IV and V of the SM). The HHG spectrum for the case of N_2 molecule is given in section IV of the SM. The amplitude and phase of the 1st to the 5th harmonics of N_2 field decomposed to the left and right circular polarization states, as a function of the alignment angle θ , are shown in Fig. 3. Due to the inversion symmetry of the molecules along their molecular axis, the response of these harmonics exhibits periodic behavior with a period of 180 degrees. Notably, several harmonic orders display an almost linear dependence of the phase on the alignment angle. This characteristic is crucial for achieving integer values of OAM in the far-field radiation generated by the molecular ensemble.

To corroborate the simulations, we developed a mathematical model describing the linear response of a diatomic molecule to a BCCP Field (see SM). We observed a good agreement of the results of this analytical theoretical calculation with the simulation results. Moreover, we observed that the fundamental and second harmonic show a value much smaller than one for the ellipticity, which is attributed to the anisotropy of the molecular polarizability tensor. This is further analyzed in the SM.

Next we present the results of far-field radiation from the macroscopic molecular ensemble. The dipole radiation from each molecule in a radially aligned ensemble is used to compute the overall far-field radiation. The field for each harmonic order q was calculated at a distance of $10 \times \lambda_q$, where λ_q is the wavelength of the q^{th} harmonic. The molecules were arranged on five concentric circles with equal spacing between each circumference. In this configuration, the outermost radius was of the order of the harmonic wavelength. The configuration of the molecular ensemble is depicted in Fig. 1.

The molecular ensemble was subjected to three different field configurations: a linear bi-chromatic field, a clockwise BCCP, and a counterclockwise BCCP field. These latter two fields were created using circularly polarized components, with the helicity switched between the two cases to explore the effects of field helicity on the far-field radiation patterns.

We then analyzed the far-field radiation patterns for several high harmonic frequencies. The fields were decomposed into a finite basis of Laguerre-Gauss modes, which are useful in evaluating the OAM possessed by a given field. This decomposition involved projecting the field onto the first 45 modes, spanning azimuthal indices $l = -4$ to $l = 4$ and radial indices $p = 0$ to $p = 4$.

The mathematical form of these modes, in cylindrical coordinates (r, ϕ, z) is:

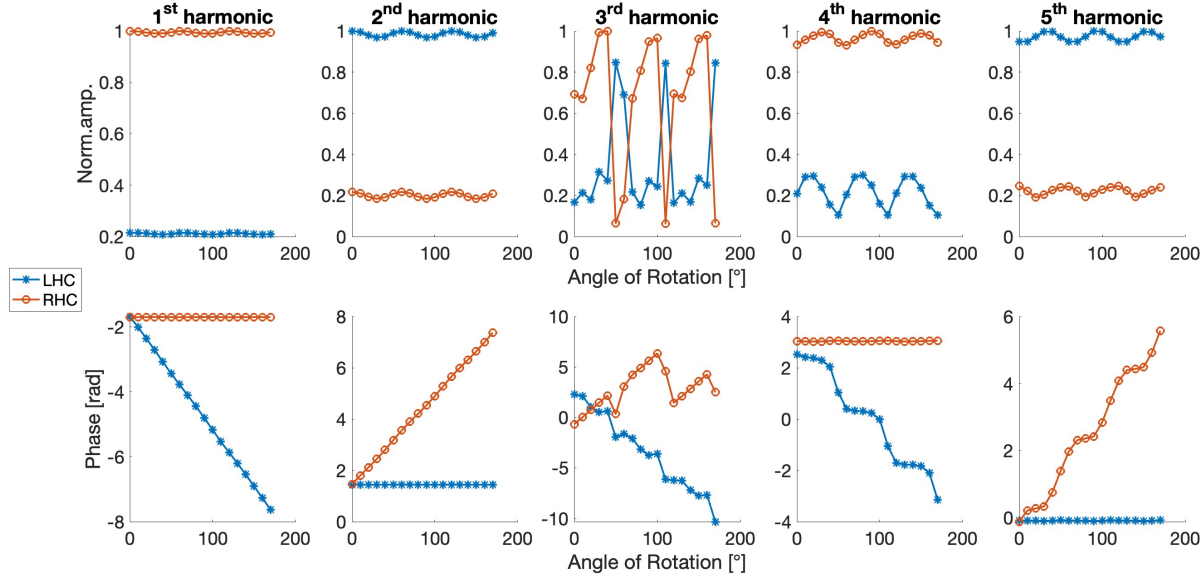


FIG. 3. Normalized amplitude (divided by the maximal value) and phase of the 1st–5th harmonics of N_2 subjected to a counter-rotating bi-chromatic laser driving field for LHC (blue) and RHC (red) polarization states.

$$\psi_{lp}(r, \phi, z) = \sqrt{\frac{2p!}{\pi(|l|+p)!}} \cdot \frac{1}{w(z)} \cdot \left(\frac{\sqrt{2}r}{w(z)}\right)^{|l|} \cdot \exp\left(-\frac{r^2}{w^2(z)}\right) \cdot L_p^{|l|}\left(\frac{2r^2}{w^2(z)}\right) \cdot \exp(il\phi) \cdot \exp\left(-i\frac{kr^2}{2R(z)}\right) \cdot \exp(i(2p+|l|+1)\xi(z)), \quad (4)$$

where $L_p^{|l|}$ is the generalized Laguerre polynomial, $w(z)$ is the beam width, $R(z)$ is the radius of curvature, and $\xi(z)$ is the Gouy phase shift [38].

From the analysis of the far-field patterns, we observed that no OAM was generated under linear polarization (as an example refer to the response at the fundamental harmonic presented in section IV of the SM). This outcome is as expected because a linearly polarized field does not exhibit the necessary symmetry in its phase and amplitude distributions to impart OAM. In essence, the dipole response induced by a linearly polarized bi-chromatic field tends to maintain symmetry that does not support the generation of OAM.

Conversely, clear OAM patterns emerged when we used BCCP fields endowed with SAM. The generated OAM changes sign with the switching of the field helicity, which exemplifies the spin-orbit interaction. This phenomenon associates the angular momentum states of the photons in the driving laser field with the resultant harmonic. This shows that the system as a whole can be interpreted as a coherently controlled molecular q-plate.

For illustrative purposes, Fig.4 displays the left and right circularly polarized components of the 5th harmonic

in the far field for N_2 molecules. These figures include both amplitude and phase details for the fields and their reconstruction from 45 Laguerre-Gauss modes, spanning azimuthal indices $l = -4$ to $l = 4$ and radial indices $p = 0$ to $p = 4$. The relative contribution of each mode is displayed as a heatmap in Fig. 5. These results can be explained using an intuitive approach based on selection-rules which is given in detail in the SM. The main point of this explanation is to first treat the molecules as point-source while using SAM selection rules to determine the dominant polarization state of the emitted radiation. However, as the molecules are anisotropic, an additional polarization state would be excited. It is assumed that this additional polarization state is phase-locked to the orientation of the molecule. These assumptions, when taken for all molecules in the macroscopically ordered ensemble of the molecular q-plate, yield the correct SAM and OAM states of the emitted radiation.

Summary. We investigated macroscopic spin-orbit interaction in a radially aligned molecular gas ensemble driven by a strong helical bi-chromatic pump field. Using real-time Time-Dependent Density Functional Theory (RT-TDDFT) simulations, we demonstrated that high harmonic radiation collectively emitted from judiciously patterned ensemble of molecular orientations carries OAM whose sign depends on the pump field's helicity. This effect, observed in H_2^+ and N_2 molecules, resembles the behavior of a q-plate, enabling coherent control of the OAM of the HHG radiated beams. Our results highlight the potential for structured light generation and macroscopic spin-orbit coupling in strong-field physics and open new avenues for ultrafast light-matter interaction.

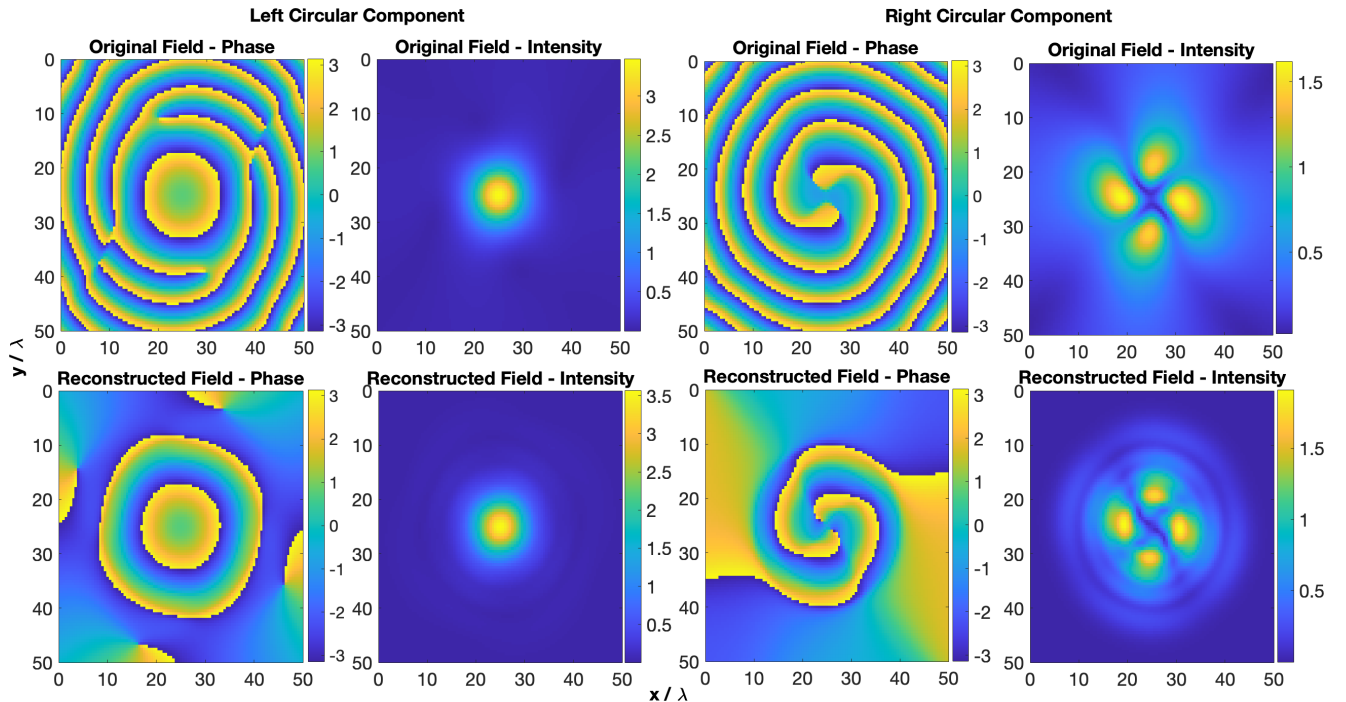


FIG. 4. Left Panel - Left circular component, Right panel - Right circular component. The upper sub-figures show the Far-field pattern of the 5th harmonic under bi-chromatic circularly polarized laser field as achieved from the simulation where the left figure shows the field's phase and the right shows the intensity. The lower sub-figures - show the "reconstructed field" composed of the sum of the first 45 LG modes 4 with the calculated coefficients. Both axes are normalized to the harmonic's wavelength.

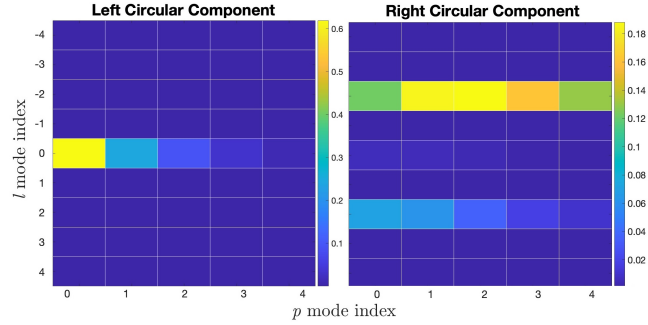


FIG. 5. Left Panel - Left circular component, Right panel - Right circular component. Decomposition of the far field pattern of the 5th harmonic under BCCP laser field into Laguerre-Gaussian modes. The indices of the modes, p and l , are arranged along the columns and rows of the image, respectively.

[1] M. Ferray, A. L'Huillier, X. Li, L. Lompre, G. Mainfray, and C. Manus, Multiple-harmonic conversion of 1064 nm radiation in rare gases, *J. Phys. B* **21**, L31 (1988).

[2] S. Ghimire and D. A. Reis, High-harmonic generation from solids, *Nat. Phys.* **15**, 10 (2019).

[3] J. Itatani, D. Zeidler, J. Levesque, M. Spanner, D. Villeneuve, and P. Corkum, Controlling high harmonic generation with molecular wave packets, *Phys. Rev. Lett.* **94**, 123902 (2005).

[4] T. Kanai, S. Minemoto, and H. Sakai, Quantum interference during high-order harmonic generation from aligned molecules, *Nature* **435**, 470 (2005).

[5] S. Ramakrishna and T. Seideman, Information content of high harmonics generated from aligned molecules, *Phys. Rev. Lett.* **99**, 113901 (2007).

[6] Y. Mairesse, J. Levesque, N. Dudovich, P. Corkum, and D. Villeneuve, High harmonic generation from aligned molecules—amplitude and polarization, *J. Mod. Opt.* **55**, 2591 (2008).

[7] C. Marceau, J. B. Bertrand, P. Peng, H. J. Wörner, P. B. Corkum, and D. M. Villeneuve, Simultaneous measurements of strong-field ionization and high harmonic generation in aligned molecules, *J. Phys. B* **53**, 084006 (2020).

[8] F. Cardano and L. Marrucci, Spin-orbit photonics, *Nat. Photonics* **9**, 776 (2015).

[9] A. Rubano, F. Cardano, B. Piccirillo, and L. Marrucci, Q-plate technology: a progress review, *JOSA B* **36**, D70 (2019).

[10] F. Trawi, F. Billard, O. Faucher, P. Béjot, and E. Hertz, Molecular quantum interface for storing and manipulating ultrashort optical vortex, *Laser Photonics Rev.* **17**, 2200525 (2023).

[11] C. Xu, L. He, W. Tao, X. Zhu, F. Wang, L. Xu, L. Xu, P. Lan, I. Averbukh, Y. Prior, *et al.*, Molecular wave plate for the control of ultrashort pulses carrying orbital angular momentum, *Phys. Rev. Lett.* **135**, 113201 (2025).

[12] A. Voisine, P. Béjot, F. Billard, O. Faucher, and E. Hertz, Molecular alignment echo for controlling the readout time of vortex beams, *Phys. Rev. Lett.* **136**, 023202 (2026).

[13] M. A. Marques, N. T. Maitra, F. M. Nogueira, E. K. Gross, and A. Rubio, *Fundamentals of time-dependent density functional theory*, Vol. 837 (Springer, 2012).

[14] E. Luppi and M. Head-Gordon, Computation of high-harmonic generation spectra of h₂ and n₂ in intense laser pulses using quantum chemistry methods and time-dependent density functional theory, *Mol. Phys.* **110**, 909 (2012).

[15] M. R. Mack, D. Whitenack, and A. Wasserman, Exchange-correlation asymptotics and high harmonic spectra, *Chem. Phys. Lett.* **558**, 15 (2013).

[16] J. Heslar, J. Carrera, D. Telnov, and S.-I. Chu, High-order harmonic generation of heteronuclear diatomic molecules in intense ultrashort laser fields: An all-electron tddft study, *Int. J. Quantum Chem.* **107**, 3159 (2007).

[17] R. Baer, D. Neuhauser, P. R. Ždánská, and N. Moiseyev, Ionization and high-order harmonic generation in aligned benzene by a short intense circularly polarized laser pulse, *Phys. Rev. A* **68**, 043406 (2003).

[18] S. Zhou, Q. Li, F. Guo, J. Wang, J. Chen, and Y. Yang, High-order harmonic generation of benzene molecules irradiated by circularly polarized laser pulses, *Chem. Phys.* **545**, 111147 (2021).

[19] A. Koushki, R. Sadighi-Bonabi, M. Mohsen-Nia, and E. Irani, High-order harmonic generation of co and n₂ molecules under linearly-and bi circularly-polarized laser pulses by td-dft, *Laser Phys.* **28**, 075404 (2018).

[20] L. Hareli, G. Shoulga, and A. Bahabad, Phase matching and quasi-phase matching of high-order harmonic generation—a tutorial, *J. Phys. B: Atomic, Molecular and Optical Physics* **53**, 233001 (2020).

[21] H. Stapelfeldt and T. Seideman, Colloquium: Aligning molecules with strong laser pulses, *Rev. Mod. Phys.* **75**, 543 (2003).

[22] S. Fleischer, Y. Khodorkovsky, E. Gershkabel, Y. Prior, and I. S. Averbukh, Molecular alignment induced by ultrashort laser pulses and its impact on molecular motion, *Isr. J. Chem.* **52**, 414 (2012).

[23] C. P. Koch, M. Lemeshko, and D. Sugny, Quantum control of molecular rotation, *Rev. Mod. Phys.* **91**, 035005 (2019).

[24] Y. Ohshima and H. Hasegawa, Coherent rotational excitation by intense nonresonant laser fields, *Int. Rev. Phys. Chem.* **29**, 619 (2010).

[25] I. S. Averbukh and N. Perelman, Fractional revivals: Universality in the long-term evolution of quantum wave packets beyond the correspondence principle dynamics, *Phys. Lett. A* **139**, 449 (1989).

[26] I. S. Averbukh and R. Arvieu, Angular focusing, squeezing, and rainbow formation in a strongly driven quantum rotor, *Phys. Rev. Lett.* **87**, 163601 (2001).

[27] M. Leibscher, I. S. Averbukh, and H. Rabitz, Molecular alignment by trains of short laser pulses, *Phys. Rev. Lett.* **90**, 213001 (2003).

[28] V. Renard, M. Renard, S. Guérin, Y. Pashayan, B. Lavorel, O. Faucher, and H.-R. Jauslin, Postpulse molecular alignment measured by a weak field polarization technique, *Phys. Rev. Lett.* **90**, 153601 (2003).

[29] F. Rosca-Pruna and M. Vrakking, Revival structures in picosecond laser-induced alignment of i₂ molecules. ii. numerical modeling, *J. Chem. Phys.* **116**, 6579 (2002).

[30] L. Kronik, A. Makmal, M. L. Tiago, M. Alemany, M. Jain, X. Huang, Y. Saad, and J. R. Chelikowsky, Parsec—the pseudopotential algorithm for real-space electronic structure calculations: recent advances and novel applications to nano-structures, *Phys. Status Solidi B* **243**, 1063 (2006).

[31] M. Mundt and S. Kümmel, Photoelectron spectra of anionic sodium clusters from time-dependent density-functional theory in real time, *Phys. Rev. B* **76**, 035413 (2007).

[32] M. Mundt, Real-time approach to time-dependent density-functional theory in the linear and nonlinear regime, *J. Theor. Comput. Chem.* **8**, 561 (2009).

[33] D. Hofmann, T. Körzdörfer, and S. Kümmel, Kohn-sham self-interaction correction in real time, *Phys. Rev. Lett.* **108**, 146401 (2012).

[34] A. Fleischer, O. Kfir, T. Diskin, P. Sidorenko, and O. Cohen, Spin angular momentum and tunable polarization in high-harmonic generation, *Nat. Photonics* **8**, 543 (2014).

[35] R. Van Leeuwen and E. Baerends, Exchange-correlation

potential with correct asymptotic behavior, Phys. Rev. A **49**, 2421 (1994).

[36] X. Chu and S.-I. Chu, Role of the electronic structure and multielectron responses in ionization mechanisms of diatomic molecules in intense short-pulse lasers: An all-electron ab initio study, Phys. Rev. A **70**, 061402 (2004).

[37] O. Neufeld, D. Podolsky, and O. Cohen, Floquet group theory and its application to selection rules in harmonic generation, Nat. Commun. **10**, 1 (2019).

[38] A. E. Siegman, *Lasers* (University science books, 1986).